Journal of Electroanalytical Chemistry 808 (2018) 372–379

Contents lists available at ScienceDirect

Journal of Electroanalytical Chemistry

journal homepage: www.elsevier.com/locate/jelechem

# Nanoconfinement of glucose oxidase on mesoporous carbon electrodes with tunable pore sizes

Conchi O. Ania[a,b,*], Alicia Gomis-Berenguer[a,b], Joseph Dentzer[c], Cathie Vix-Guterl[c]

[a] Instituto Nacional del Carbon (INCAR, CSIC), 33011 Oviedo, Spain
[b] CEMHTI, CNRS (UPR 3079) CNRS, Université d'Orléans, 45071 Orléans, France
[c] Institut de Science des Matériaux de Mulhouse (IS2M), LRC CNRS 7228, Mulhouse, France

ARTICLE INFO

*Keywords:*
Glucose oxidase
Nanoporous carbons
Nanoconfinement
Pore size distribution

ABSTRACT

By using a series of nanoporous carbons with a controlled distribution of pore sizes we have demonstrated the effect of commensurate confinement in the nanopores of the carbon electrodes in the electrochemical and enzymatic activity of immobilized glucose oxidase. The nanoconfinement resulted in more efficient oxidation of glucose through direct electron tunneling of the flavin adenine dinucleotide (FAD) site and the electrode surface. The electrochemical and enzymatic activity was boosted in carbon materials with pores which size matched the dimensions of the enzyme. This is attributed to the conformational changes of the biomolecule in the nanoconfined state, and the proximity of the FAD active site and the carbon electrode pores/walls boosts the electron transfer even in the absence of a mediator. The thermal profiles of the immobilized enzyme provided direct evidence of the conformational changes in the nanoconfined state, and their correlation with the average mesopore size of the carbon material. For the material showing the most adequate porosity, the nanoconfined enzyme retained the electrocatalytic activity towards glucose oxidation -even in the absence of mediator-, and at a broad range of concentrations. This approach is essential to make further clear some critical issues about the immobilization of enzymes on nanoporous carbon electrodes for bioelectrochemical applications.

## 1. Introduction

Besides the extensive use of graphite and carbon black as electrodes, many different types of carbon forms (i.e., graphene and derivatives, carbon nanotubes, diamond related compounds, nanofibres or nanoporous carbons) exhibiting varied bulk, structural and surface properties have been extensively explored as main components in the formulation of carbon-based inks for electrochemical applications [1–3]. Particularly in the field of electrochemical biosensing, nanoporous carbon-based electrodes offer interesting opportunities due to their physicochemical features that combine mechanical and chemical stability, biocompatibility, relatively high conductivity and mostly importantly, reproducible up-scale synthesis for mass production of electrochemical devices [4–7].

Nanoporous carbons (NPC) as electrodes allow a quick and accurate monitoring of a pool of metabolites due to the enhanced stability of the confined molecules inside the pores. Thus, the choice of a carbon material as electrode may not only be dictated by parameters such as electron transfer rates, stability, mass transfer limitations and/or redox potentials, but also by its textural characteristics (in terms of surface area, pore volume and distribution of pore sizes) that control the host-guest interactions, and thus the stability of the nanoconfined molecule. NPC are thus ideal electrode materials for the design of third generation electrochemical sensors and biosensors based on achieving direct electron transfer (DET) processes between the electrode surface and the immobilized molecules [8–12]. The key aspect of such biosensors is to achieve improved selectivity and lower redox potentials, while preserving the stability of the immobilized molecules, since DET allows the measurement of the substrate of the enzyme without the need of mediators or complications associated to solution system [13–14].

However, the redox/active sites of most enzymes are often deeply buried within the protein, hindering direct electron transfer communication between the enzyme and the electrode surface. This is the case, for instance of glucose oxidase (GOX), where the flavin adenine dinucleotide (FAD) moiety, is deeply embedded in the protein shell of GOX. Immobilization on porous supports is perhaps the simplest alternative to overcome these drawbacks; however, this scenario may become quite complex, since the immobilization can induce conformation changes on the biomolecule that would reduce its enzymatic activity, even if direct electrical transfer at the electrode surface is achieved [15–17]. Indeed,

* Corresponding author at: CEMHTI-CNRS (UPR 3079), Université d'Orléans, 45071 Orléans, France.
*E-mail address:* conchi.ania@cnrs-orleans.fr (C.O. Ania).

http://dx.doi.org/10.1016/j.jelechem.2017.09.009
Received 31 March 2017; Received in revised form 2 August 2017; Accepted 6 September 2017
Available online 07 September 2017

understanding the confinement of immobilized molecules on nanopore spaces is still challenging.

The objective of this work was to explore the utilization of NPC with a varied distribution of pore sizes in the mesoporous range, to investigate the impact of nanoconfinement of glucose oxidase on such electrodes on the long term stability and enzymatic response for glucose biosensing. To attain this goal, nanoporous carbon gels prepared by sol-gel polycondensation of resorcinol-formaldehyde mixtures were used as electrode materials for the immobilization of the enzyme. These materials can be easily synthesized with tunable pore architectures by adjusting the synthesis conditions [18–21], thus allowing to obtain carbons combining large specific surface areas with a proper network of transport pores to favor the diffusion and adsorption of bulky molecules [22,23]. The novelty of the work resides on providing a deep insight on the role of the tight nanoconfinement of an immobilized enzyme inside the porosity of carbon electrodes, aiming at correlating the electrochemical and enzymatic response with the pore dimensions of the carbon-based electrode materials. This approach is essential to make further clear some critical issues about the immobilization of enzymes on nanoporous carbon electrodes in bioelectrochemical applications.

## 2. Experimental

### 2.1. Materials and reagents

All chemicals were of analytical reagent grade and were used without further purification. Glucose oxidase (E.C. 1.1.3.4, from Aspergillus niger), glucose d-(+)-glucose (97%) and ferrocene monocarboxylic acid were obtained from Sigma-Aldrich. Nafion perfluorinated ion-exchange (5 wt% solution in 90% alcohol) was obtained from Fluka. GOX was dissolved in phosphate buffer saline (PBS) solution (0.1 M, pH = 7.6) and stored at 4 °C until use (concentrations ranging from 10–200 μM).

### 2.2. Synthesis of the carbon materials

Nanoporous carbon gels were synthesized by the sol-gel polymerization of resorcinol (R) and formaldehyde (F) in water (W), using sodium carbonate (C) as catalyst, as reported elsewhere [20,21]. Briefly, the precursors were mixed at fixed molar ratios (R/W of 0.06, R/F of 0.5 and R/C of 50, 75, 100 and 200) under magnetic stirring and immediately heated in airtight sealed glass vessels for gelation/aging at 95 °C for 4 h in an oven. Afterwards, the wet gels were dried at subcritical conditions at 150 °C for 12 h, and further carbonized at 800 °C under inert atmosphere (i.e., 100 mL/min $N_2$) for 1 h. Different R/C molar ratios (50, 75, 100 and 200) were used to obtain carbon gels with varied porous features in the mesoporous range. The carbon gels were labeled as Gx, where x refers to the R/C molar ratio (i.e., G50, G75, G100 and G200). The carbon gels were dried at 80 °C overnight and kept in desiccator until use. A commercial carbon black (Super P, TIMCAL) was also used as electrode material for comparison purposes. The nomenclature of this sample was CB.

### 2.3. Preparation of the inks and electrodes

About 10 mg of solids were dispersed in 5 mL of isopropyl alcohol by sonication; about 20 μL of this ink were casted onto a 3 mm glassy carbon (GC) electrode (previously polished with 0.05 μm alumina slurry) and allowed to dry at room temperature. A Nafion binder film (ca. 5 μL of 5 wt% Nafion aqueous solution) was subsequently deposited on top of the electrode to facilitate the cohesion between the glassy carbon support and the casted ink. The electrodes were then immersed in ca. 20 mL of 0.1 M PBS containing 10 mg/mL of GOX at 4 °C, for 24 h. To remove the weakly bounded enzyme, the electrodes were rinsed several times with distilled water and PBS solution. The casted electrodes were labeled as GC/Z, where Z stands for the NPC material (Gx or CB), and GC/Z/GOX when the enzyme is immobilized on the carbon materials. Free GOX was also casted directly onto the glassy carbon electrode to evaluate the activity of the enzyme on the bare non-porous support. The electrodes were stored at 4 °C in a refrigerator when not used.

### 2.4. Electrochemical measurements

All the electrochemical measurements were carried out at room temperature in a three electrode configuration cell, using the prepared working electrodes casted on the GC support, a Pt wire as counter electrode and a calomel SCE reference electrode -via Luggin probe-. Deoxygenated 0.1 M PBS solutions were used in all the cases (ca. bubbling $N_2$ for 30 min and additionally maintaining a $N_2$-rich atmosphere over the solution). Due to the nanoporous nature of the carbon materials, the electrodes were immersed in 0.1 M PBS buffer solution for at least 6 h prior to the measurements so as to guarantee the access of the electrolyte to the pores (wettability), and then stabilized a few cycles. The electrochemical response of the electrodes was evaluated by cyclic voltammetry at 20 mV/s in a multichannel potentiostat/galvanostat. For evaluating the electrocatalytic response of the immobilized GOX, cyclic voltammograms were recorded in the absence and presence of ferrocene monocarboxylic acid as mediator, in a potential range between −1000 and 1200 mV. The linearity of the electrocatalytic response of the best performing electrode after subsequent injections of glucose was recorded in the presence (ca. + 350 mV) and absence (ca. + 900 mV) of mediator.

### 2.5. GOX adsorption

Glucose oxidase adsorption capacity of the studied carbon materials was determined by UV–Vis spectrophotometry from aqueous solution. Briefly, about 50 mg of the carbons were dispersed in a PBS solution of glucose oxidase and allowed to equilibrate for 24 h under continuous stirring. The carbon is then filtered out and the concentration of the enzyme remaining in the solution was determined by UV–Vis spectrophotometry. The amount of GOX adsorbed was calculated from the mass balance of the amount of enzyme remaining in the solution.

### 2.6. Characterization techniques

The porous features of the carbon materials were evaluated by $N_2$ adsorption/desorption isotherms at −196 °C using a volumetric analyzer (ASAP 2010, Micromeritics). The samples were degassed at 120 °C for 17 h under vacuum before the analysis. Each isotherm was performed in duplicate (error was below 2%). Ultrahigh purity nitrogen (i.e., 99.995%) was supplied by Air Products. The gas adsorption data was used to determine the specific surface area, $S_{BET}$, total pore volume, $V_{PORES}$ and full micro-/mesopore size distribution of the samples, the latter using the 2D-NLDFT-HS model assuming pore surface heterogeneity [24].

The interactions of the immobilized enzyme on the carbon gels were investigated using Temperature Programmed Desorption coupled to mass spectrometry (TPD-MS) in a custom-made device. Briefly, the samples were put in a fused-silica reactor and heated up to 873 K (heating rate 2 °C/min) under vacuum. The gases evolved were detected online by the mass spectrometer, recording several *m/z* simultaneously. Before the analysis, the carbon materials were loaded with the enzyme and washed several times to eliminate the weakly adsorbed biomolecule, as indicated above. The blanks corresponding to the carbon gels before the immobilization of the protein were also recorded.

Samples were chemically characterized by elemental analysis; the materials were dried under vacuum at 393 K for 17 h before the analysis. The contents of carbon, hydrogen, and nitrogen were measured in a LECO CHNS-932 microanalyzer (ASTM D-5373). The oxygen content

**Table 1**
Elemental analysis (wt% on dry basis) and main textural parameters of the NPC obtained from the equilibrium $N_2$ adsorption/desorption isotherms at − 196 °C.

| | G50 | G75 | G100 | G200 | CB |
|---|---|---|---|---|---|
| $S_{BET}$ [$m^2 g^{-1}$] | 836 | 853 | 849 | 827 | 41 |
| $V_{PORES}$[a] [$cm^3 g^{-1}$] | 0.76 | 0.89 | 1.01 | 1.25 | 0.13 |
| $V_{MICRO}$[b] [$cm^3 g^{-1}$] | 0.23 | 0.23 | 0.24 | 0.22 | n.e. |
| $V_{MESO}$[b] [$cm^3 g^{-1}$] | 0.50 | 0.63 | 0.76 | 1.02 | n.e. |
| $V_{MESO}/V_{PORES}$ [%] | 69 | 73 | 76 | 82 | n.e. |
| $S_{external}$[c] [$m^2 g^{-1}$] | 255 | 263 | 267 | 262 | 18 |
| Carbon content (wt%)[d] | 97.9 | 97.9 | 97.9 | 98.7 | 98.7 |
| Hydrogen content (wt%)[d] | 0.8 | 0.8 | 0.9 | 0.7 | 0.8 |
| Oxygen content (wt%)[d] | 1.4 | 1.4 | 1.2 | 0.6 | 0.5 |

n.e. not evaluated.
[a] Total pore volume evaluated at $p/p_0 \sim 0.99$.
[b] Micropore/mesopore volumes evaluated from DFT.
[c] Surface outside the micropores [25] evaluated from DFT.
[d] Elemental analysis on dry ash-free basis.

was independently measured in a LECO VTF-900 instrument.

## 3. Results and discussion

### 3.1. Characterization of the nanoporous carbons

The effect of the various synthesis parameters -such as the molar ratio of reactants, pH, surfactant concentration, aging temperature- on the textural and morphological features of carbon gels has been widely discussed in the literature [18–21], and remains out of the scope of this study. We herein introduce the main physicochemical parameters of the prepared NPC used as electrodes for the immobilization of GOX for data interpretation and aiming at elucidating the role of nanopore confinement on the activity of the immobilized enzyme.

The series of NPC was chosen on the basis of their textural properties and composition (Table 1). All of them displayed a high carbon content and basic surface pH, characteristic of carbon materials with a low surface functionalization degree. This is important since it allows isolating the effect of nanopore confinement of the enzyme on its electrochemical and enzymatic activity, disregarding other contributions arising from specific interactions (that would eventually lead to the degradation of the immobilized enzyme).

As for the textural properties, all the carbon gels displayed type IVa nitrogen isotherms with prominent hysteresis loops in the desorption branch at relative pressures above 0.4, characteristic of micro/mesoporous solids (Fig. 1) [25]. Despite the overall similarities in the shape of the nitrogen adsorption isotherms of the NPC, outstanding differences were observed regarding the total pore volumes, and most importantly, the position of the hysteresis loops (Table 1). For instance, sample G50 presented a H2(a) loop with a steep desorption at $p/p_0 \sim 0.5$, indicating the existence of ink-bottle shaped mesopores connected to the external surface through narrow necks [26–28]. Samples G75, G100 and G200 showed hysteresis loops featuring at higher relative pressures compared to G50, and with adsorption and desorption branches gradually becoming somewhat parallel with rising the R/C molar ratio. This is associated the presence of larger mesopores with more uniform bodies -i.e., larger mean size than those of G50-, connected through necks with size distributions similar to the width of the main cavities [25].

The main textural parameters (e.g., surface area and pore volumes) of the nanoporous carbon gels obtained from the analysis of the gas adsorption data are compiled in Table 1. Data corresponding to the carbon black is also included for comparison. All the carbon gels displayed similar values of BET surface area and micropores volumes, whereas the total pore volumes increased with the R/C molar ratio. This behavior is a common characteristic of this type of carbon materials obtained from sol-gel polycondensation of RF mixtures [18–21].

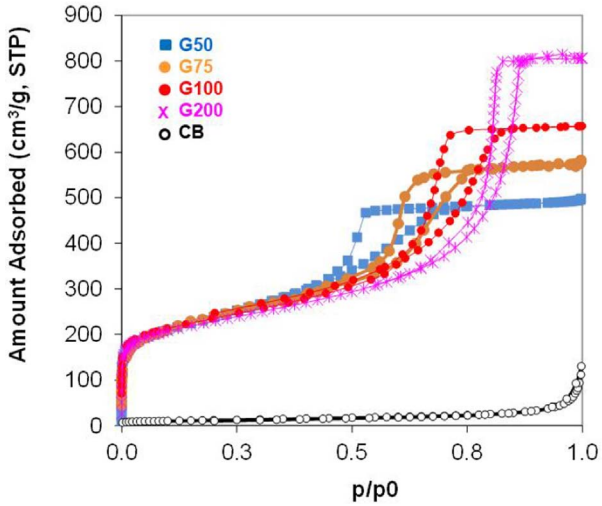


**Fig. 1.** High resolution equilibrium $N_2$ adsorption isotherms at − 196 °C of the studied nanoporous carbons.

Interestingly, all the gels exhibited a large contribution of mesopores to the overall porosity (ranging from ca. 70–80%). Consequently, the contribution of the external surface ($S_{external}$) for the NPC is quite large, and similar for all of them (Table 1). On the other hand, the carbon black is a non-porous electrically conductive electrode material, as inferred from the main textural parameters shown in Table 1.

The differences in the porosity of the studied carbons are more clearly seen in the analysis of the pore size distributions (PSD) and pore volumes obtained in the full micro-mesopore range (Fig. 2). It should be pointed out that PSD profiles have been obtained by the 2D-NLDFT-HS method applied to both the adsorption and desorption branches of the nitrogen adsorption isotherms. This is recommended in the literature for a realistic characterization of complex pore systems where percolation effects might apply [26–28], as it is the case of herein reported materials. In these cases, the information obtained from the adsorption branch of the nitrogen isotherm provides a realist distribution of the size of the mesopore bodies; on the other hand, the analysis of the desorption branch may be applied to gather information about the size of the pore neck.

As seen, all the carbon gels displayed similar distributions in the micropore range, with larger micropore volumes than those of the carbon black. This is in agreement with the overlapped shapes of the adsorption isotherms of all the carbon gels in the low relative pressures range (ca. below 0.2). Although the exact dimensions of glucose oxidase are still uncertain (they depend on many parameters as the confinement state, the nature of the surface, or the humidity, among most representative), values for the dimeric structure fall within the mesoporous range (ca. 7 × 5.5 × 8 nm for the dimer) [29,30]. The immobilization of GOX is expected to occur on pores which size commensurate the dimensions of the enzyme: the surface outside the micropores, so-called external surface. Thus, the slight differences in the microporosity of the samples are not expected to be relevant for the immobilization of GOX.

Indeed, it should be mentioned that, even if some enzymes can somehow distort to accommodate in pores of dimensions close or slightly lower than their molecular dimensions, GOX is quite a rigid molecule [31], and only pores with sizes equal or higher to its dimensions are expected to be accessible to the enzyme. Thus the focus of the textural analysis should be paid to the mesoporosity of the samples. Furthermore, the external surface area is quite small for the carbon black (ca. 18 $m^2/g$) compared to the carbon gels that showed similar values (ranging between 255 and 270 $m^2/g$, Table 1). These porous features allow investigating the effect of nanoconfinement upon the mesopore size of the carbon support.

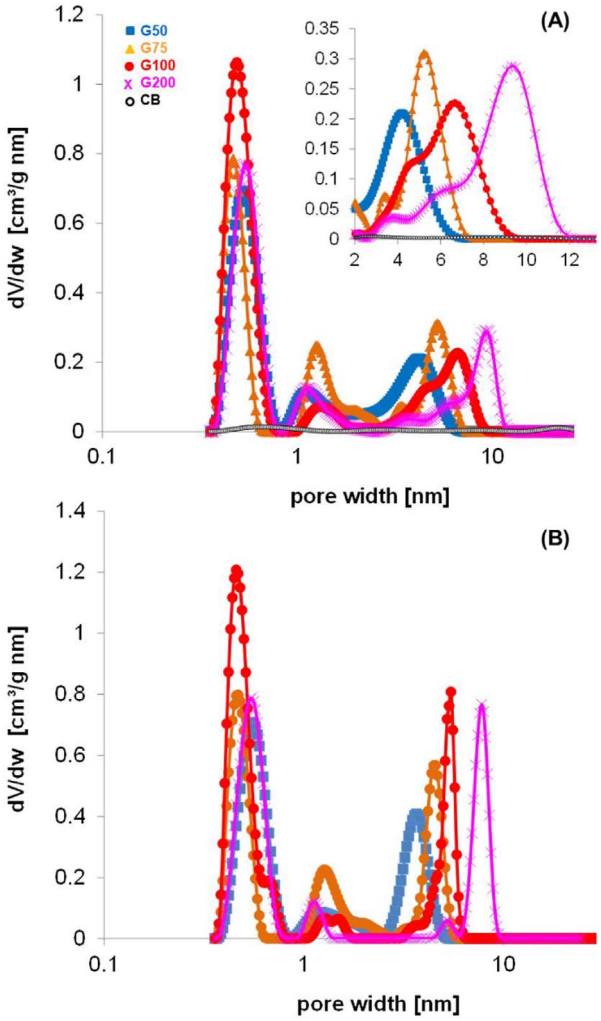


**Fig. 2.** PSD of the nanoporous carbons obtained from the nitrogen isotherms at − 196 °C by application of the 2D-NLDFT-HS method to the adsorption (A) and desorption (B) branch. Inset: magnification of the PSD corresponding to the adsorption branch.

As mentioned above, all the carbons showed an outstanding contribution of mesopores to the overall pore volume (Table 1), with marked differences in the actual mesopore volume and average widths. The PSD obtained from both the adsorption and desorption branches were quite narrow for all the samples and followed the same trend in terms of mean pore size, with values slightly higher for the former. In both cases, the average mesopore size followed the trend: G50 < G75 < G100 < G200 (Fig. 2). This indicates that for all the carbon gels, the mesoporosity is comprised of main cavities larger in diameter than the pore apertures connecting them. This is going to have a strong impact on the immobilization on the enzyme, as it will be discussed below.

### 3.2. Electrochemical behavior of the GC/NPC/GOX electrodes

Fig. 3 shows the cyclic voltammograms (CVs) of the GC/NPC and GC/NPC/GOX electrodes in a $N_2$-saturated phosphate buffer solution (0.1 M, pH 7). The profiles corresponding to the nanoporous carbons (series of electrodes GC/NPC) showed a wide quasi-rectangular shape over the registered potential range, due to the contribution of the capacitive current in porous materials (Table 1). The voltammograms of the GC/NPC electrodes were quite similar for all the carbon gels, which is in good agreement with their similar micropore volumes (Table 1) since the main contribution to the double layer capacitance arises from microporosity [3]. This is also an indication of the good dispersion of the nanoporous carbon-based inks, leading to homogenous casting on the GC support. The current recorded for the GC/CB electrode was much lower than that of the GC/NPC electrodes, as expected based on the lower porous features of the carbon black.

The immobilization of the enzyme (GC/NPC/GOX electrodes) did not cause significant changes in the capacitive contribution of the voltammograms compared to the GC/NPC electrodes; this suggest the lack of pore blockage arising from an inadequate immobilization of the biomolecule in the external surface area of the carbons, that would eventually block the inner porosity (seen as capacitive current drop). It should also be mentioned that no faradaic peaks were detected for GOX directly casted on the bare glassy carbon electrode, indicating that this support is not a suitable medium for observing direct electron transfer between the enzyme and the electrode surface. Similar findings have been reported in the literature for glassy carbon electrodes [10,14].

Notably, the immobilization of glucose oxidase on the carbon black (electrode GC/CB/GOX) produced an enhancement in the faradaic current (the capacitive current remained low), with two well-defined anodic and cathodic peaks observed at ca. − 470 and − 436 mV vs SCE, respectively. The cathodic and anodic peak currents were equal and nearly symmetrical indicating the quasi-reversibility of the electrochemical reaction of GOX immobilized in the carbon black. These values are close to those reported in the literature for the electronic transfer between the flavin adenine dinucleotide (FAD/FADH2) at pH 7 [9,12]. This confirmed that the immobilization of GOX on the external surface area of the carbon black facilitates the electron exchange between the electroactive center of glucose oxidase and the support. The positive effect on the electron transfer has been reported for GOX immobilization on various carbon blacks, mesoporous silica or carbon nanotubes, among others [9–12,32,33].

A different behavior was obtained for the immobilization on the NPC. The faradaic peaks corresponding to the direct electron tunneling between FAD and the electrode surface were clearly detected for GC/G75/GOX and GC/G100/GOX electrodes; in contrast, the intensity of the peaks was much lower for GC/G200/GOX, and not detected in the case of GC/G50/GOX. This is most remarkable considering that the electrical conductivity of the carbon gels (ca. 0.4–0.6 S/m) is several orders of magnitude lower that than of the carbon black (ca. $10^4$ S/m), and points out the intimate interaction of the enzyme inside the pores of carbon gels G75 and G100. The confinement of the enzyme inside the nanopores of the carbon material may lead to conformational changes of the biomolecule, which are expected to affect the electronic coupling at the carbon electrode/enzyme interface. This may also affect the activity of the immobilized enzyme for glucose sensing, since an adequate orientation of the biomolecule is essential for an efficient electron transfer.

In the case of samples G50 and G200, the lack of the faradaic peaks after the immobilization of the enzyme may be associated to various phenomena such as a poor immobilization of the enzyme in the pore structure, an inadequate orientation of the enzyme in the pores, current losses due to limited conductivity of the electrodes, or dilution effects due to the large capacitive contribution, among most representative.

To identify the origin of this behavior, adsorption studies were carried out to quantify the adsorption capacity of the carbons towards GOX using batch experiments in solution consisting in dispersing the carbons in a PBS solution of glucose oxidase, and measuring the concentration remaining in solution after equilibration (Fig. 4). This approach eliminates eventual errors arising from the immobilization of the enzyme on the glassy carbon support due to uneven casting of the inks. Data revealed interesting information regarding the correlation between the immobilization of the enzyme and the porous network of the carbon materials.

As seen, the amount of GOX adsorbed on sample G50 was almost negligible compared to the uptake of the rest of nanoporous carbons, including the carbon black. This behavior must be attributed to the porous features of this carbon gel (Table 1). As mentioned above, the

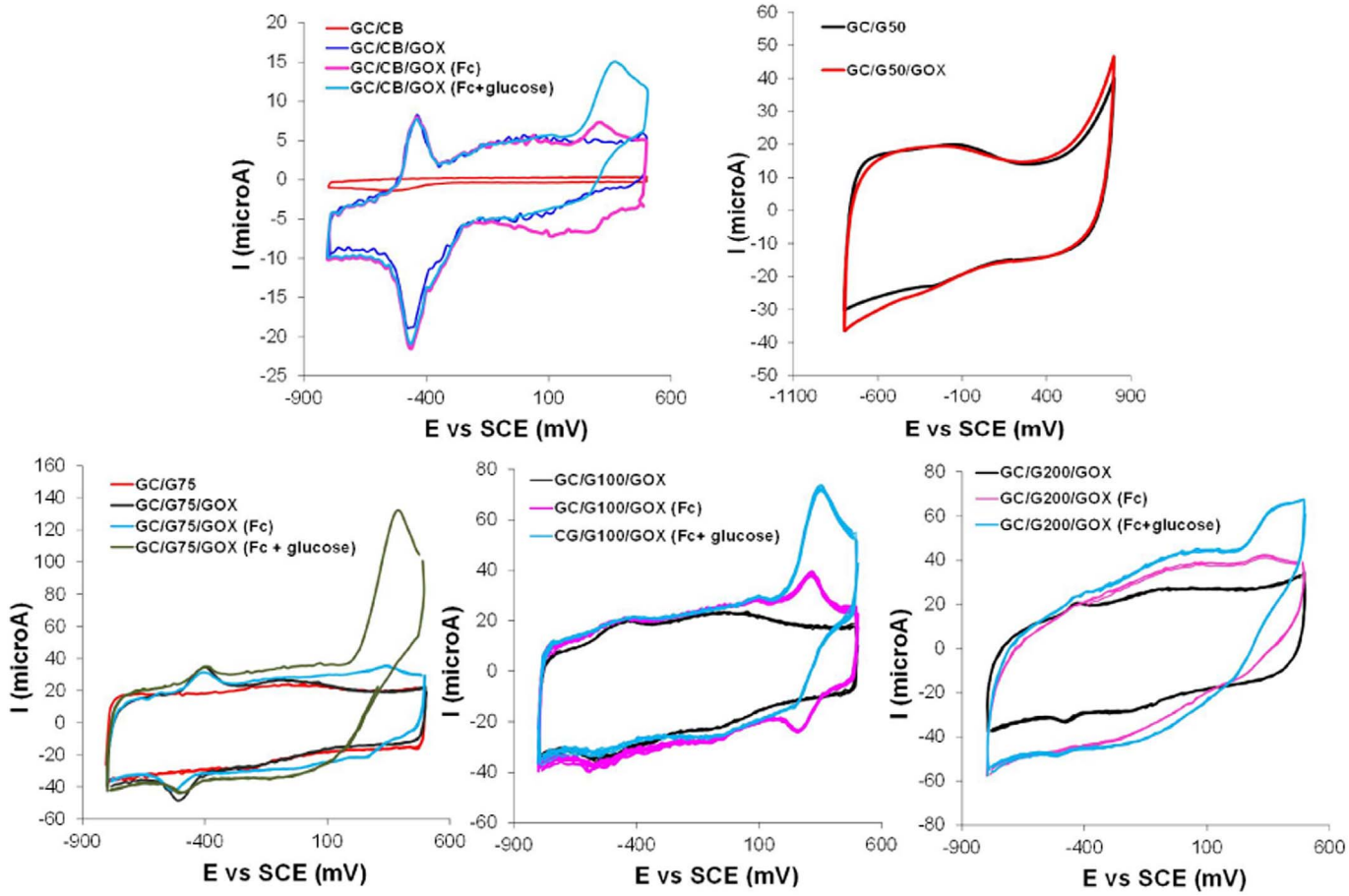


**Fig. 3.** Cyclic voltammograms of the GC/NPC/GOX electrodes in a $N_2$-saturated phosphate buffer solution (0.1 M, pH 7) in the presence and absence of ferrocene monocarboxylic acid (Fc) mediator, and glucose.

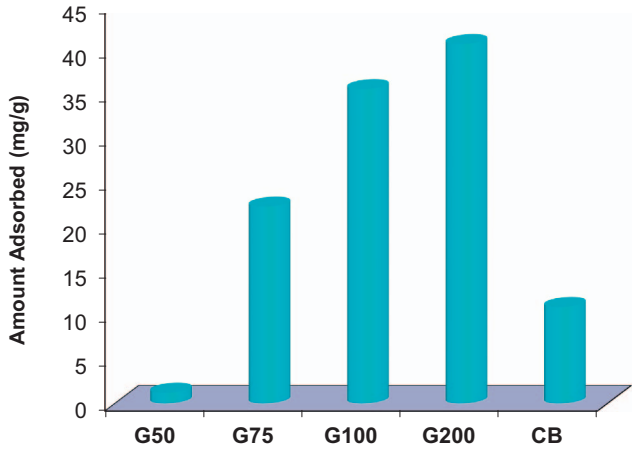


**Fig. 4.** Adsorption capacity of glucose oxidase in the nanoporous carbons.

analysis of the pore size distribution of sample G50 by means of gas adsorption showed that this particularly carbon displayed a narrow distribution of mesopores centered at about ca. 4 nm, connected through smaller pore mouths of ca. 3.5 nm (Fig. 2). Such small dimensions of the pore openings prevent the glucose oxidase, hence its immobilization in the inner mesopore network. There some studies in the literature on the use mesoporous carbons as supports for GOX, reporting successful immobilization on carbons with ordered structure and pore diameters of about 4.1 and 4.2 nm [34]. This suggests that 3.5 nm is a threshold pore aperture value for the immobilization of glucose oxidase on nanoporous materials.

On the other hand, the mesoporous network of G75, G100 and G200 are also narrow but the mesopores are accessible due to presence of larger pore necks (Fig. 2) that enable the diffusion of GOX to the main mesopore cavities. Accordingly, the enzyme uptake is high and increased with the pore volume (Fig. 4). In contrast, the low uptake of the carbon black must be associated to its low porosity (Table 1), and the enzyme is adsorbed on its external surface, which as opposed to G50 corresponds to open pores accessible to the enzyme.

All this confirms that the absence of faradaic peaks in the voltammograms of the GC/G50/GOX electrode is attributed to the inadequate size of the pore apertures of this carbon, which prevents the immobilization of the enzyme (the surface outside the micropores is not accessible to GOX). This cannot be the case for G200, where it should be most likely linked to either the low conductivity of this carbon (seen in the shape of the voltammograms), to conformational changes of the biomolecule inside the pores (eventually leading to the loss of the enzymatic activity), or to the shielding effect of the large capacitive current of this electrode.

In sum, having a well-developed pore structure within the mesopore range does not grant a successful immobilization of a bulky molecule such as GOX unless the pores commensurate the dimension of the molecules, thereby assuring the diffusion inside the pores. Besides uptake, the confinement of the enzyme in the nanopores of the carbon electrode may lead to conformational changes of the biomolecule depending on the size of the pores. This is expected to affect the electronic coupling at the carbon electrode/enzyme interface, and may also affect the electrocatalytic and/or enzymatic activity of the immobilized enzyme for glucose sensing.

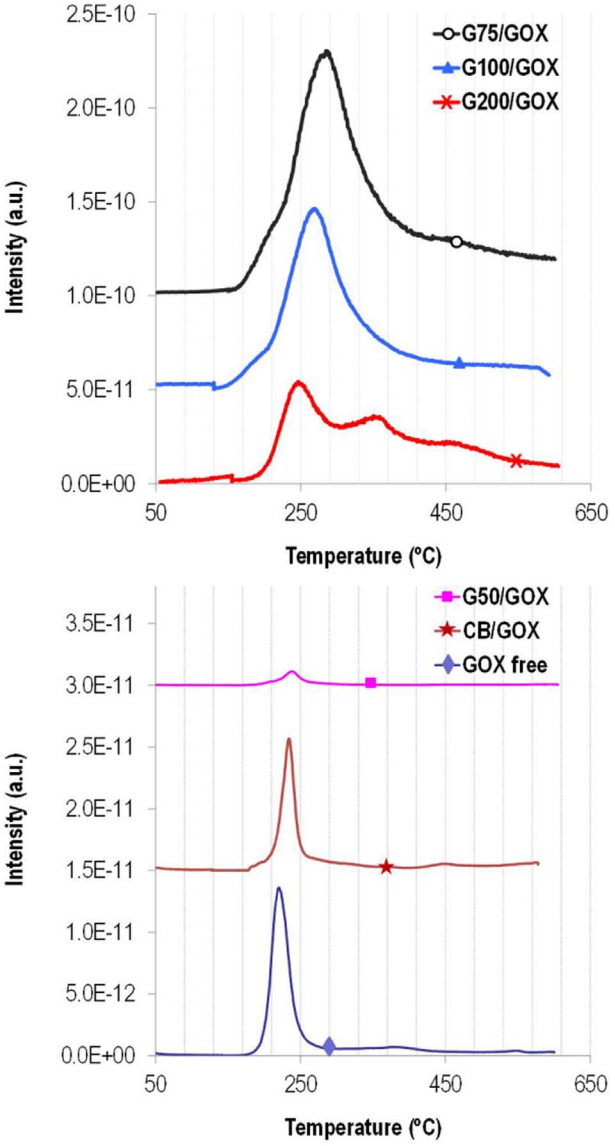


**Fig. 5.** TPD-MS signal of the fragment *m/z* 34 formed during decomposition of the free and adsorbed enzyme in the nanoporous carbon samples.

The conformation state and stability of the nanoconfined GOX was investigated by TPD-MS, based on the temperature of the desorbed species evolved in the thermal profiles of the carbon materials after the immobilization of the enzyme (Fig. 5). This approach has been validated for the quantification of the proteins adsorption capacity on carbon adsorbents, as well as to explore the interactions between the protein and the carbon surface [35,36]. It is important to point out that to eliminate interferences arising from the decomposition of the surface groups of the carbon materials (mostly desorbed as CO and $CO_2$), the decomposition of the enzyme was followed through the *m/z* 34 (corresponding to the decomposition of sulfur containing amino acids), which is not present in any of the carbon samples (Table 1).

For the non-adsorbed protein (in solution) the thermal decomposition mainly occurred at 220 °C (sharp peak), followed by a small tail above 300 °C. The profiles corresponding to the desorption of the enzyme immobilized on the NPC followed a complex wider pattern, with differences in the desorption onset and the number of peaks, depending on the nanoporous carbon. Compared to the free protein, the onset of the main desorption peak appeared at higher temperatures for the immobilized enzyme. We attribute these shifts to conformational changes likely induced by the interactions between the nanoconfined enzyme

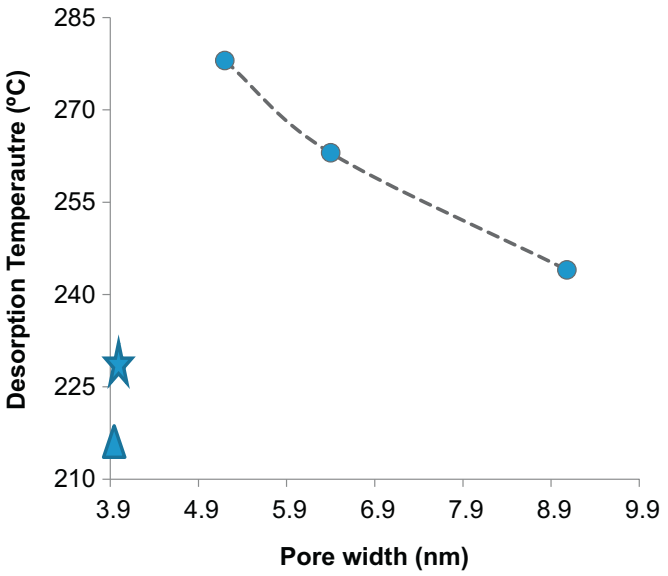


**Fig. 6.** Correlation between the desorption temperature in the TPD-MS profiles and the mean pore size of the carbons (adsorption branch). Data corresponding to the decomposition of the enzyme in solution (triangle) and immobilized in the carbon black (star) is also plotted for comparison purposes.

and the surface of the carbons. This is also an indication that the protein is in a more stable conformation after adsorption on a nanoporous carbon than in a flat surface (free solution), and that the stability of the nanoconfined molecule depends on the nanoporous carbon. Similar results have been reported for the immobilization of glucose oxidase on carbon nanotubes, silica, or tridimensional graphene-like materials [10,16,32,37].

The profile corresponding to the immobilization on G50 displayed a low signal and the onset desorption temperature was close to that obtained upon the immobilization on the carbon black. This was rather expected considering the low uptake of GOX of this sample, and corroborates that the protein does not enter the pores but is adsorbed to a very small extent in the external surface area of this sample. On the other hand, the profile of sample G200 featured various desorption peaks, which are attributed to multiple conformational states of GOX nanoconfined in the porosity of this carbon (i.e., multiple interactions of the protein with the pore walls).

Another interesting observation is that these differences in temperature can be straightforwardly correlated to the confinement state and the size of the pores. Fig. 6 shows the gradual decrease of the desorption temperature (first peak in the case of G200) with rising the mean pore size of the carbons. This indicates the higher stability of the enzyme in the tight confinement in carbon G75, where the size of the pores matches the dimensions of the protein.

Based on the composition of the carbons, the interactions of the enzyme inside the pores are mainly dispersive in nature; hence, the driving force of the conformational changes would originate from the tight confinement of the biomolecule inside pores of adequate size and the accommodation with different orientations. When GOX is adsorbed on the carbons, the hydrophobic core of the enzyme would be prone locate near the hydrophobic carbon pore walls, leaving the more hydrophilic FAD active center facing the entrance of the pores. This confirms that the tight confinement in pores that commensurate the molecular size of the enzyme facilitates the electron transfer.

The conformation of the FAD in apo-GOX may also affect the activity of the enzyme; thus in order to discriminate whether if the immobilized enzyme retains its enzymatic activity towards the oxidation of glucose, the electrocatalytic response of the electrodes to successive additions of glucose was investigated. The electrochemical response was recorded in the presence and absence of a non-physiological

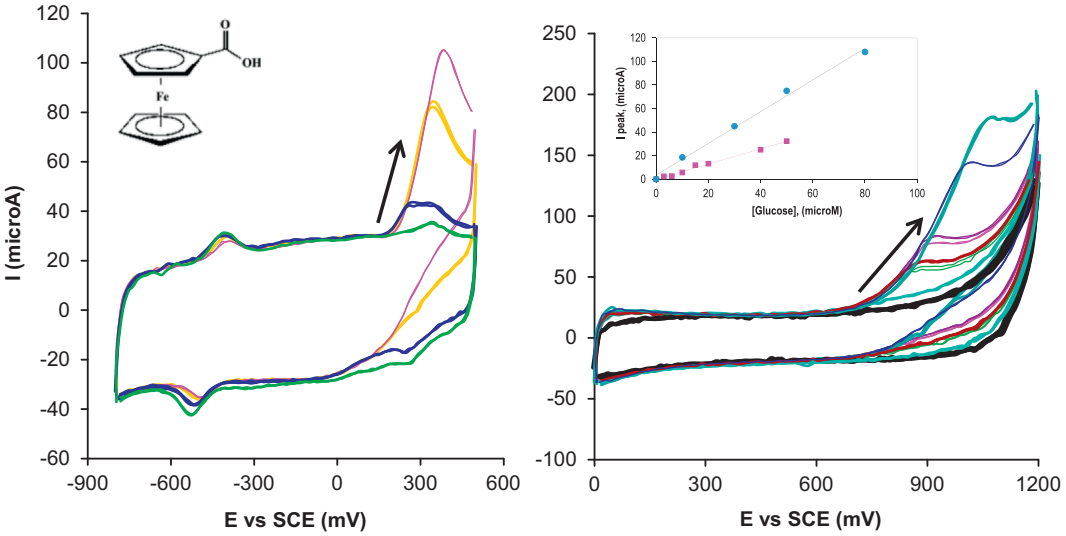


**Fig. 7.** Cyclic voltammograms of GC/G75/GOX electrode in a $N_2$-saturated phosphate buffer solution (0.1 M, pH 7) upon addition of increasing amounts of glucose (indicated by arrows) in the presence (left) and absence (right) of the mediator. Inset: representation of the linearity of the response in the absence (squares) and presence (circles) of the mediator.

mediator (ferrocene derivative), to facilitate the electron shuttle between the FAD center and the electrode surface. It is also important to point out that all the measurements were recorded on solutions under an inert environment to remove oxygen.

With the exception of CB/G50/GOX, the voltammograms of all the studied electrodes showed two broad waves (anodic peak at ca. + 350 mV and cathodic peak at + 270 mV) corresponding to the characteristic reversible redox process of ferrocene monocarboxylic in solution [38]. This confirmed that, even though a mediator is needed to boost the electronic coupling at the electrode surface, the electrochemical activity is maintained despite the likely new conformational states of the enzyme adsorbed on CB, G75, G100 and G200.

Fig. 7 shows the anodic peak currents of GC/G75/GOX electrode with increasing glucose concentration and in the presence and absence of ferrocene. The current at + 350 mV corresponding to the redox reactions of the mediator increased with the concentration of glucose (while the peaks corresponding to FAD redox transitions remained unchanged), confirming the effective diffusion of glucose through the nanoporous carbon matrix towards the active catalytic center of GOX. Interestingly, the electrode also showed some electrocatalytic activity in the absence of the mediator, as observed by the increased current at around + 870 mV (Fig. 7). This points out that the immobilized enzyme retains the catalytic activity based on direct electron transfer reactions at the nanoporous carbon/enzyme interface.

Furthermore, the electrocatalytic current for glucose detection in the presence of the mediator followed a linear response to the substrate in the range of glucose concentrations 10–80 μM (inset Fig. 7), reaching saturation at values above 160 μM. These values are quite acceptable compared to the performance of other configuration of glucose oxidase immobilized on various carbon electrodes [11,14,34,39], even though the optimization of nanoporous carbons as electrode materials for glucose biosensing was not the scope of this work. The stability and reproducibility of the stability of the GC/G75/GOX electrode were also evaluated after various week storage in PBS at 4 °C. After 10 days, the response of the stored electrodes in 0.1 M PBS in the presence of the mediator retained 94% value of the initial response of the newly fabricated electrodes. This implies that the GC/G75/GOX electrode is stable upon time and efficient for retaining the bioactivity of enzyme.

## 4. Conclusions

Owing to the recently gained interest on the use of nanoporous carbons as electrodes in electrochemical applications, we have used a series of carbon gels with well-defined pore architectures for gaining a fundamental understanding of the impact of nanoconfinement and the biomolecule/pore interactions on the electron transfer rate and electrocatalytic activity of the immobilized enzyme.

Matching of the molecular dimensions of the biomolecule to be immobilized with the size of the nanopores of the carbon electrode is a valuable strategy for the preparation of glucose oxidase-confined carbon-based electrodes. Data showed that immobilization on carbon hosts of adequate dimensions and good electrical conductivity results in conformational changes in the adsorbed molecule that facilitate the direct electron transfer with the electrode surface due to the proximity and adequate orientation of the active redox center in the constrained pore space. The dimensions of the main nanopore cavities are important to define the orientation and stability of the nanoconfined enzyme, which are essential to maintain the electrocatalytic activity through a direct electron transfer process. On the other hand, the size of the pore openings also plays a crucial role as it controls the diffusion (accessibility) of the enzyme to the inner porous network of the carbon host.

We have shown the importance of tuning the pore dimensions of carbon electrodes for the immobilization of enzymes. Selected carbon gels with large surface area and a uniform mesoporous network were demonstrated as more suitable candidates than carbon black to immobilize glucose oxidase and promote heterogeneous electron transfer. Furthermore, the immobilization on carbon G75 showed a stable electrocatalytic response towards the oxidation of glucose over time, as well as a linear response for a large range of glucose concentrations (quite remarkable in the absence of a mediator); these features arise from the commensurate confinement of the enzyme on the carbon support with adequate pore structure. This approach provides an essential experimental base for the understanding of the electrochemistry of redox proteins in confined systems, while evaluating the potential application of nanoporous carbons for the immobilization of enzymes. We anticipate that tuning the porosity of carbon electrodes opens up an interesting strategy towards the development of third generation biosensors based on non-mediated reactions.

## Acknowledgments

COA thanks the financial support of the European Research Council through a Consolidator Grant (ERC-CoG-648161, PHOROSOL), the Spanish MINECO through an excellence network E3TECH (grant CTQ2015-71650-RDT), and CNRS for a mobility action (poste rouge).

## References


[1] L. Zhu, C. Tian, D. Yang, X. Jiang, R. Yang, Bioanalytical application of the ordered mesoporous carbon modified electrodes, Electroanalysis 20 (2008) 2518–2525.
[2] C. You, X. Yan, J. Kong, D. Zhao, B. Liu, Bicontinuous gyroidal mesoporous carbon matrix for facilitating protein electrochemical and bioelectrocatalytic performances, Talanta 83 (2011) 1507–1514.
[3] K. Kinoshita, Carbon: Electrochemical and Physicochemical Properties, Wiley, 1988.
[4] J. Iniesta, L. Garcia-Cruz, A. Gomis-Berenguer, C.O. Ania, Carbon materials based on screen printing electrochemical platforms in biosensing applications, Electrochemistry Series, RSC Publishing, 2016, pp. 133–169.
[5] J.P. Smith, J.P. Metters, D.K. Kampouris, C. Lledo-Fernandez, O.B. Sutcliffe, C.E. Banks, Forensic electrochemistry: the electroanalytical sensing of Rohypnol® (flunitrazepam) using screen-printed graphite electrodes without recourse for electrode or sample pre-treatment, Analyst 138 (2013) 6185–6191.
[6] S.C. Wang, K.S. Chang, C.J. Yuan, Enhancement of electrochemical properties of screen-printed carbon electrodes by oxygen plasma treatment, Electrochim. Acta 54 (2009) 4937–4943.
[7] M. Pagan, D. Suazo, N. del Toro, K. Griebenow, A comparative study of different protein immobilization methods for the construction of an efficient nano-structured lactate oxidase-SWCNT-biosensor, Biosens. Bioelectron. 64 (2015) 138–146.
[8] B. Haghighi, M.A. Tabrizi, Direct electron transfer from glucose oxidase immobilized on a nano-porous glassy carbon electrode, Electrochim. Acta 56 (2011) 10101–10106.
[9] C.-H. Xue, R.-J. Zhou, M.-M. Shi, G. Wu, X.-B. Zhang, M. Wang, H.-Z. Chen, Electrochemistry of glucose oxidase immobilized on carbon nanotubes non-covalently functionalized by multihydroxyl and multicarboxyl groups, J. Eletroanal. Chem. 642 (2010) 92–97.
[10] K. Wang, H. Yang, L. Zhu, J. Liao, T. Lu, W. Xing, S. Xing, Q. Lv, Direct electrochemistry and electrocatalysis of glucose oxidase immobilized on glassy carbon electrode modified by Nafion and ordered mesoporous silica-SBA-15, J. Mol. Catal. B Enzym. 58 (2009) 194–198.
[11] K. Wang, H. Yang, L. Zhu, Z. Ma, S. Xing, Q. Lv, J. Liao, C. Liu, W. Xing, Direct electron transfer and electrocatalysis of glucose oxidase immobilized on glassy carbon electrode modified with Nafion and mesoporous carbon FDU-15, Electrochim. Acta 54 (2009) 4626–4630.
[12] Y.D. Zhao, W.D. Zhang, H. Chen, Q.M. Luo, Direct electron transfer of glucose oxidase molecules adsorbed onto carbon nanotube powder microelectrode, Anal. Sci. 18 (2002) 939–941.
[13] C. Cai, J. Chen, Direct electron transfer of glucose oxidase promoted by carbon nanotubes, Anal. Biochem. 332 (2004) 75–83.
[14] L. Wang, J. Bai, X. Bo, X. Zhang, L. Guo, A novel glucose sensor based on ordered mesoporous carbon-Au nanoparticles nanocomposites, Talanta 83 (2011) 1386–1391.
[15] C.Q. Chi, J. Zhang, S. Dong, E. Wang, Direct electrochemistry and surface characterization of glucose-oxidase adsorbed on anodized carbon electrodes, Electrochim. Acta 39 (1994) 2431–2438.
[16] F. Liu, X.-S. Ye, T. Wu, C.-T. Wang, J.-W. Shen, Y. Kang, Conformational mobility of GOx coenzyme complex on single-wall carbon nanotubes, Sensors 8 (2008) 8453–8462.
[17] D. Wen, Y. Liu, G. Yang, S. Dong, Electrochemistry of glucose oxidase immobilized on the carbon nanotube wrapped by polyelectrolyte, Electrochim. Acta 52 (2007) 5312–5317.
[18] S.A. Al-Muhtaseb, J.A. Ritter, Preparation and properties of resorcinol-formaldehyde organic and carbon gels, Adv. Mater. 15 (2003) 101–114.
[19] N. Job, R. Pirard, J. Marien, J.-P. Pirard, Porous carbon xerogels with texture tailored by pH control during sol-gel process, Carbon 42 (2004) 619–628.
[20] G. Rasines, P. Lavela, C. Macias, M.C. Zafra, J.L. Tirado, C.O. Ania, Mesoporous carbon black-aerogel composites with optimized properties for the electro-assisted removal of sodium chloride from brackish water, J. Electroanal. Chem. 741 (2015) 42–50.
[21] E.D. Isaacs-Peaz, M. Haro, E. Juarez-Perez, R.J. Carmona, J.B. Parra, R. Leyva-Ramos, C.O. Ania, Fast synthesis of micro/mesoporous xerogels: textural and energetic assessment, Microporous Mesoporous Mater. 209 (2015) 2–9.
[22] C.D. Liang, Z.J. Li, S. Dai, Mesoporous carbon materials: synthesis and modification, Angew. Chem. Int. Ed. 47 (2008) 3696–3717.
[23] W. Xin, Y.H. Song, Mesoporous carbons: recent advances in synthesis and typical applications, RSC Adv. 5 (2015) 83239–83285.
[24] J. Jagiello, J.P. Olivier, Carbon slit pore model incorporating surface energetical heterogeneity and geometrical corrugation, Adsorption 19 (2013) 777–783.
[25] M. Thommes, K. Kaneko, A.V. Neimark, J.P. Olivier, F. Rodriguez-Reinoso, J. Rouquerol, K.S.W. Sing, Physisorption of gases, with special reference to the evaluation of surface area and pore size distribution (IUPAC technical report), Pure Appl. Chem. 87 (2015) 1051–1069.
[26] M. Thommes, K.A. Cychosz, Physical adsorption characterization of nanoporous materials: progress and challenges, Adsorption 20 (2014) 233–250.
[27] J. Landers, G.Y. Gor, A.V. Neimark, Density functional theory methods for characterization of porous materials, Colloids Surf. A: Physicochem. Eng. Asp. 437 (2013) 3–32.
[28] P.I. Ravikovitch, A.V. Neimark, Experimental confirmation of different mechanisms of evaporation from ink-bottle type pores: equilibrium, pore blocking, and cavitation, Langmuir 18 (2002) 9830–9837.
[29] D. Rando, G.W. Kohring, F. Giffhorn, Production, purification and characterization of glucose oxidase from a newly isolated strain of *Penicillium pinophilum*, Appl. Microbiol. Biotechnol. 48 (1997) 34–40.
[30] S. Libertino, V. Aiello, A. Scandurra, M. Renis, F. Sinatra, Immobilization of the enzyme glucose oxidase on both bulk and porous $SiO_2$ surfaces, Sensors 8 (2008) 5637–5648.
[31] S. Hosseinkhani, A.A. Moosavi-Movahedi, M. Nemat-Gorgani, Interaction of glucose oxidase with alkyl-substituted Sepharose 4B, Appl. Biochem. Biotechnol. 110 (2003) 65–74.
[32] H. Li, J. He, Y. Zhao, D. Wu, Y. Cai, Q. Wei, M. Yang, Immobilization of glucose oxidase and platinum on mesoporous silica nanoparticles for the fabrication of glucose biosensor, Electrochim. Acta 56 (2011) 2960–2965.
[33] T.E. Benavidez, D. Torrente, M. Marucho, C.D. Garcia, Adsorption and catalytic activity of glucose oxidase accumulated on OTCE upon the application of external potential, J. Colloid Interface Sci. 435 (2014) 164–170.
[34] C. You, X. Xu, B. Tian, J. Kong, D. Zhao, B. Liu, Electrochemistry and biosensing of glucose oxidase based on mesoporous carbons with different spatially ordered dimensions, Talanta 78 (2009) 705–710.
[35] M. Vijayaraj, R. Gadiou, K. Anselme, C. Ghimbeu, C. Vix-Guterl, H. Orikasa, T. Kyotani, S.K. Ittisanronnachai, The influence of surface chemistry and pore size on the adsorption of proteins on nanostructured carbon materials, Adv. Funct. Mater. 20 (2010) 1–11.
[36] R. Gadiou, E.A. dos Santos, M. Vijayaraj, K. Anselme, J. Dentzer, G.A. Soares, C. Vix-Guterl, Temperature-programmed desorption as a tool for quantification of protein adsorption capacity in micro- and nanoporous materials, Colloids Surf. B: Biointerfaces 73 (2009) 168–174.
[37] V.R. Gonçales, R.N.P. Colombo, M.A.O.S. Minadeo, E.Y. Matsubara, J.M. Rosolen, S.I. Córdoba de Torresi, Three-dimensional graphene/carbon nanotubes hybrid composites for exploring interaction between glucose oxidase and carbon based electrodes, J. Electroanal. Chem. 775 (2016) 235–242.
[38] A. Harper, M.R. Anderson, Electrochemical glucose sensors-developments using electrostatic assembly and carbon nanotubes for biosensor construction, Sensors 10 (8) (2010) 8248–8274.
[39] L. Jia, G. Lawrence, V.V. Balasubramanian, G. Choi, J.-H. Choy, A.M. Abdullah, A. Elzatahry, K. Ariga, A. Vinu, Highly ordered nanoporous carbon films with tunable pore diameters and their excellent sensing properties, Chem. Eur. J. 21 (2015) 697–703.